令和 5 年度 修士論文

Properties evaluation of short carbon fiber reinforced aluminum matrix composites fabricated by spark plasma sintering method

指導教員佐々木 元教授

広島大学大学院工学研究科 機械物理工学専攻

材料物理学研究室

M215747

Murugan Chairmanraja

Abstract

Metal matrix composites (MMCs) are lightweight metal alloys made of titanium, magnesium, or aluminum that have been strengthened with ceramic fibers, whiskers, or particles. The reinforcement is crucial since it affects the composite's mechanical characteristics, price, and performance. Because of qualities like reduced weight, increased stiffness, and superior thermal conductivity, aluminum composites are popular materials for application in engineering disciplines like aerospace, automotive, and mineral processing industries. Typically, glass, ceramic, and carbon fibers are used in the fabrication of aluminum composites as reinforcement materials. In terms of mechanical qualities and wear resistance, aluminum metal matrix composites reinforced with fibers offer great and extremely rewarding potential. The 99.9% pure aluminum that is used in this study has a diameter of 3μm, and the short carbon fiber that serves as a reinforcement material has a length of 6mm and a diameter of 11μm. Aluminum was reinforced with 1% and 2% volume fractions of carbon fibers at various temperatures. Carbon fibers were cleaned of impurities to avoid agglomeration. The pot mill rotating table was used for ball milling method. It was used to combine the pure aluminum with the carbon fiber. The blended powder was fabricated using the spark plasma sintering method, and then the mechanical properties of the resulting composites were examined. The effect of the temperature on the properties of the composites such as morphology, thermal conductivity, hardness, and relative density were studied and compared.

Contents

Chapter 1 Introduction

1.1 Research Background

Thermal management materials and heat dissipation materials are crucial and important for compact electronic devices used in aerospace and for heat sink applications in hybrid vehicles. The temperature of the components should be kept low so that thermal management materials can be used to dissipate the heat produced by CPUs or semiconductor devices or engine applications to the surroundings or atmosphere [1-2].

As thermal management and heat dissipation materials, metals, particularly copper and aluminum, are employed. However, it has disadvantages such as low strength and low rigidity, as well as a high thermal expansion coefficient. Due to the inadequacy of metals and alloys to provide sufficient strength and rigidity, Metal Matrix Composites (MMC) are created and developed. The metal matrix, which is the base material, provides the strength and ductility factors, while the reinforcement, which can be ceramic or metal-based fibers with high stiffness, provides the stiffness factors.

MMCs are manufactured by dispersing reinforcing material throughout a metal matrix. Reinforcements for non-metallic inorganic components must meet the requirements of low density, mechanical compatibility, chemical compatibility, thermal ability, high young's modulus, high compression and tensile strength, good process ability, and economic efficiency, whereas reinforcements for metal matrix composites must meet the requirements of high density and affinity to the matrix. MMCs have properties such as a low thermal expansion coefficient and a high thermal conductivity that make them suitable for use in electronic packaging applications.

Aluminum composites are chosen for applications involving lightweight metals. Due to their light weight and superior thermal conductivity, aluminum matrix composites are the engineering material of choice in the aerospace and automotive industries for a variety of applications [3]. In addition, it has a high tensile strength, Young's modulus, is easy to shape, is inexpensive, and has excellent wear and corrosion resistance. Carbon materials such as carbon fiber and carbon nanofiber are gaining popularity and are regarded as efficient reinforcement in advanced composites with favorable mechanical properties [4-5]. Carbon fiber-reinforced aluminum matrix composites have the majority of desirable properties for use in heat management applications, including low coefficient of thermal expansion (CTE), high electrical/thermal conductivity, high specific strength, and good wear resistance. Carbon fiber-reinforced composites have been extensively utilized in a variety of applications, including aircraft brakes, space structures, military and commercial aircraft, lithium batteries, sporting goods, and structural reinforcement [6].

Carbon nanofibers (CNF/CF) are allotropes of carbon arranged in hexagonal lattice. Carbon nanofibers are cylindrical nanostructures with graphene layers arranged as stacked cones, cups, or plates. Reinforcing the ductile Aluminum matrix with carbides provides large improvements in

physical and mechanical properties of the composites [7]. Vapor-grown carbon fiber (CF) is also tubular type carbon nanotube (CNT) which is used in the study [8]. Young's modulus and the tensile strength of the CNT and CF are more than 5 times of steel and weight is as small as 1/5. Conventional sintering process which is one of the Powder metallurgy methods which is chosen to fabricate this composite [9].

1.2 Metal matrix composites fabrication methods

Metal matrix composites can be created in a variety of ways. Different approaches are used for various needs due to factors such as cost control, complexity of preparation, and shape and size of the final product. Both liquid and solid processes are commonly used in the preparation process. Powder metallurgy and stir casting are the two primary types of solid processes, while there are three primary types of liquid processes. It is often not possible to make the final product from scratch. Therefore, after-treatment plays a significant role in the preparation of metal matrix composites in order to meet varying requirements.

1.2.1 Liquid Process

The liquid process is a method of preparation that has the benefits of being inexpensive, having an easy preparation process, and being able to prepare complex products. The interfacial reaction between the metal and the reinforcing base is encouraged by the high temperature needed for the preparation using the liquid method, but this significantly reduces the mechanical properties of the composite. Furthermore, the distribution of the filler when using the liquid process is more strongly influenced by the wettability between the filler and the matrix than when using the solid process. Coating the filler's surface is a common technique for solving the interface problem. When using the liquid method, coating the reinforcing substrate can increase the wettability of the metal while controlling the fabrication process parameters is to get a well-distributed composite. Another issue is that the filler may float or settle in the molten metal because the density of the reinforcing matrix is different from that of the metal, making it very challenging to create a composite that is homogeneous and evenly distributed.

1.2.1.1 Liquid metal infiltration

Liquid metal infiltration is a process in which molten metal is forced under pressure through a solid pattern until it fills the holes and then waits to solidify. This process of preparation consists of only two steps: Model preparation and metal extrusion into the porous model [10].

1.2.1.2 Stir casting

In stir casting, reinforcement is incorporated into the molten metal and heated during stirring [11]. Stir casting has attracted a lot of interest from the industry due to its ease of use and low cost when compared to other fabrication techniques. It is challenging to produce a uniformly distributed

composite material using this technique, and its use is constrained by the drawbacks of strong interfacial reaction and insufficient wettability.

1.2.2 Solid Process

Metal matrix composites are frequently prepared using the solid process. Without a phase transition, composite materials can be made directly in a solid state at a lower temperature than during a liquid process. Additionally, composite materials' structures are simpler to manage.

1.2.2.1 Powder metallurgy

The most popular solid method for creating metal matrix composites is powder metallurgy. It is a cost-effective method for creating high-performance metal matrix composites, which can combine different materials and have relatively unique properties. In addition to stir casting, powder metallurgy can be used to create composite materials with more unique structures.

In powder metallurgy, the sintering procedure is a crucial step that largely determines how the material's structure is controlled. The two primary methods of powder metallurgy sintering are hot pressing and spark plasma sintering [12-14].

1.2.3 Spark plasma sintering

In recent years, spark plasma sintering has become a popular sintering technology. It offers a number of significant benefits over conventional sintering. The sample can be heated evenly at a high heat rate using this method. Additionally, the samples can be sintered for a brief period of time at a very low temperature to produce small grain samples. The production efficiency is higher for SPS. In addition to temperature and pressure, plasma in an electric field also acts as the driving force of SPS. As a result, SPS makes it simple to obtain samples with higher densities. This method can also be used to prepare composite materials, metals, ceramics, porous materials, and metals. This technology will become more crucial to the development of new materials as it is promoted and used more widely [15].

1.3 Carbon Fibers and its role in metal matrix composites

CF is a carbon-based fiber that is derived from coal tar pitch, a byproduct of the coal coking process. CF has garnered considerable interest and application in the field of metal matrix composites (MMC) due to its unique properties and reinforcement potential. The role of CF in enhancing the mechanical and thermal properties of MMCs, as well as its applications in various industries, have been investigated in prior research.

CF's high strength-to-weight ratio is a significant advantage, making it an excellent candidate for reinforcing metal matrices. The incorporation of CF into metal matrices, such as aluminum, magnesium, or titanium, has been shown to significantly improve the composites' mechanical properties. The high tensile strength and modulus of CF contribute to the increased stiffness and load-

bearing capacity of MMCs, making them suitable for applications that require lightweight and high-performance materials.

In addition, CF possesses superior thermal stability and resistance to harsh environments, making it suitable for applications involving elevated temperatures or thermal cycling. The inherent heat resistance of CF enables the creation of MMCs that can withstand extreme conditions, such as those found in the aerospace, automotive, and energy industries. The thermal stability and mechanical strength of CF make it a desirable reinforcement option for MMCs in high-temperature applications [8].

In addition to its mechanical and thermal properties, interfacial bonding between CF and metal matrices has been investigated in previous research. Interfacial adhesion between the fiber and matrix is essential for transferring loads and optimizing the overall performance of the composite. Various surface modification techniques, such as chemical treatments, coatings, and functionalization techniques, have been investigated to improve interfacial bonding. These methods are intended to enhance the fiber-matrix interface and ensure efficient stress transfer within composite structures [9].

Multiple studies have demonstrated the effective incorporation of CF into MMCs and their application in a variety of fields. Due to their exceptional thermal properties, CF-based MMCs have been investigated as potential materials for thermal management systems and heat exchangers.

In conclusion, previous research emphasizes the significance of CF in metal matrix composites. Its high strength-to-weight ratio, thermal stability, and interfacial properties help to improve the mechanical and thermal performance of MMCs. Utilization of CF in the field of MMCs will be advanced by continued research and development aimed at optimizing fiber-matrix interactions and investigating novel applications.

1.4 Purpose of Research

The present study summarizes the work carried out in the field of short carbon fiber reinforced aluminum matrix composites (AMCs). These composites are being projected for use in automobile, aerospace, and structural applications for their high specific strength as well as functional properties such as exciting thermal and electrical conductivity. The present study focuses on the critical and important issues faced by CF reinforced AMCs that includes the processing techniques like spark plasma sintering method, and by Ultrasonification process, ball milling process, strengthening mechanisms like hardness and mechanical properties. Coal tar pitch carbon fiber is provided from Mitsubishi Chemical Corporation and Aluminum is provided from Kojundo Chemical Laboratory Co.

The objective of this experiment is to determine the optimal powder-mixing conditions for producing composites with greater relative density and enhanced thermal conductivity. Also, the relative density, orientation of carbon fibers, and volume fraction so the influence of these factors on the thermal conductivity of the material is discussed. Also, the work focuses on the study about the effect of the temperature on the properties of the composites such as morphology, thermal conductivity, hardness, and relative density.

Chapter 2 Experiment Procedures

2.1 Introduction

In this chapter, the base material (Al), reinforcement material (CF) used in the fabrication of the cylindrical samples are presented. All geometries were fabricated by using Spark Plasma Sintering (SPS) method.

2.2 Preparation of CF/Al

The present study analyses the effect of 1% and 2% short of carbon fibers (CF) addition on the Al composites where Aluminum is 99.9% pure which is used as the matrix material and CF as the reinforcement material. Table 2.1 shows the shapes and the properties of CF of Al powder used in the present study.

Table 2.1 Shape and Physical Properties of Al Powder and CF [16]

Shape and physical properties	**CF**	**Al**
Average diameter, *d*/μm	11	3
Fiber length, *L*/mm	6	-
True density, ρ/Mg · m^{-3}	2.2	2.7
Thermal conductivity/W· $m^{-1} \cdot K^{-1}$	550	237
Coefficient of thermal expansion, α/× $10^{-6}K$	-1.45~7	23

To mix the Al powder with CF uniformly,

- CF is treated in Ultrasonication.
- CF/Al is mixed in the Ball milling mixer.

2.3 Ultrasonification

The phenomenon of Van der Waals force of attraction plays a significant role in material science, particularly in the context of agglomeration and its implications on enhancing material properties. When particles come into close proximity, these weak intermolecular forces lead to the formation of aggregates, known as agglomerates. Unfortunately, these agglomerates can restrict the desired improvement of material properties, thereby posing challenges in material engineering.

To address the issue of agglomeration and its adverse effects on material properties, various

techniques are employed. One such technique is the utilization of an ultrasonication machine, which is employed before the ball milling process and acid treatment. The underlying principle of ultrasonication revolves around the use of ultrasonic vibrations, typically within the frequency range of 20-40 kHz, to agitate a fluid. This mechanical agitation created by the ultrasonic waves helps in the separation of particles and mitigates the formation of agglomerates.

The success of the ultrasonication process largely depends on the choice of surfactant, solvent, and reagent. These chemical agents influence the degree of particle separation and, subsequently, the prevention of agglomeration. By using appropriate solvents in conjunction with ultrasonication, the surface conditions of the material, such as coal tar pitch fibers (CFs), can be significantly improved. This enhanced surface condition not only minimizes agglomeration but also curtails re-bonding of particles, which is crucial for achieving desirable material properties.

It is worth noting that the use of ultrasonication can be versatile, ranging from employing water as the medium to incorporating solvents tailored to suit the specific cleaning requirements. This adaptability ensures efficient particle separation and cleaning based on the nature of the material and contaminants to be removed. The duration of ultrasonic cleaning varies depending on the object under consideration and typically ranges between three to six minutes. However, for more complex objects or heavily agglomerated materials, the ultrasonication process might extend beyond 20 minutes to ensure thorough cleaning and separation.

In the context of the Ultrasonification process, the unzipping process of individual CFs from their bundles takes place. The shear stress induced by the ultrasonic waves plays a pivotal role in the separation of these particles, thereby enhancing the dispersion of CFs in the medium. As a result, the CFs exhibit improved homogeneity and are less prone to agglomeration. Moreover, the CFs have the propensity to absorb some of the solvents used in the Ultrasonification process, further enhancing their surface characteristics.

Overall, the use of ultrasonication as a pre-treatment technique holds immense promise in material engineering, particularly for materials like coal tar pitch fibers. By effectively addressing the issue of agglomeration, ultrasonication contributes to the production of nanocomposites with enhanced mechanical properties and functionalities. The meticulous choice of surfactants, solvents, and reagents ensures that the ultrasonication process is optimized to deliver the desired material properties. Furthermore, ultrasonication serves as an efficient cleaning method, removing contaminants from materials and objects, making it an indispensable tool in various industrial and scientific applications.

2.4 Ball milling

The Nitto Kagaku.co. pot mill rotating table ANZ-51S was used to combine the CF and aluminum powder. By breaking up the reinforcement into smaller pieces, ball milling enables a better and more uniform dispersion of reinforcement into the composite. During ball milling, the process control agent (PCA) has a significant impact on the morphological evolution of powders. CF is added to ethanol prior to the ball milling process for ultrasonic stirring to ensure uniform distribution and

avoid particle agglomeration. Ethanol is added to stop cold welding. CF is then added to the aluminum powder in the aluminum container in the following step. The mixture was then supplemented with ethanol and 10 mm steel balls, with a charge ratio of 1:10 and 1 being a mixed powder. Ethanol was added to the ball milling process as a solvent to prevent powder breakage and because it won't evaporate as quickly as methanol and acetone. The tiny rigid balls collide during the ball milling process in a concealed container. It functions according to the impact and attrition principle. The concealed aluminum container was kept on the rotating table of the milling machine. The aluminum container is placed and rotates in the opposite direction from the rotating table. Ball milling was done for three hours at various rotations per minute. The difference in the rotations per minute is to show how the powder reacts with the variable of rotating speed. The powder mixture and milling balls inside the container are subjected to the centrifugal forces produced by the rotation of the container around its own axis and the rotation of the rotating table. In theory, the impact force created in the container by the steel balls used to crush the particles should cause the powders to become finer. Because the materials inside the container rotate in the opposite direction from the rotating table of the machine, the impact force is generated when the powder particles strike the container's inner wall. For the uniform distribution of the powder, various conditions are tested.

These are the various types:

- 240 rotations per minute (Al + 1% CF and Al + 2% CF)
- 320 rotations per minute (Al + 1% CF and Al + 2% CF)
- 400 rotations per minute (Al + 1% CF and Al + 2% CF)

Fig 2.1 Nitto Kagaku.co. pot mill rotating table ANZ-51S.

2.5 Fabrication of the composite material by Spark plasma sintering

Spark plasma sintering is a technology that was developed recently with the use of industrial machinery, but it has a much older history. This technology uses a high heating rate and pressure to uniformly heat samples. Additionally, the sample can be sintered at a low temperature for a shorter period of time to produce grains with a smaller size. Spark plasma sintering has a high production efficiency as a result. This technology can be used to create materials with complex shapes, including metal, ceramic, nanomaterials, amorphous materials, composite materials, and gradient materials. Figure 2.2 displays a schematic representation of the spark plasma sintering apparatus. Spark plasma is similar to hot pressing, but it uses a completely different heating technique. It is a pressure sintering technique that conducts sintering directly using electric current. Discharge plasma, discharge shock pressure, Joule heat, and electric field diffusion are the primary functions of electric current. Particle discharge, conductive heating, and pressurization all work together to produce spark plasma sintering. The surface of the particles may melt and peel off as a result of the effective discharge between the particles, which can result in localized high temperatures [17]. Thus, it is possible to create composites with high relative densities.

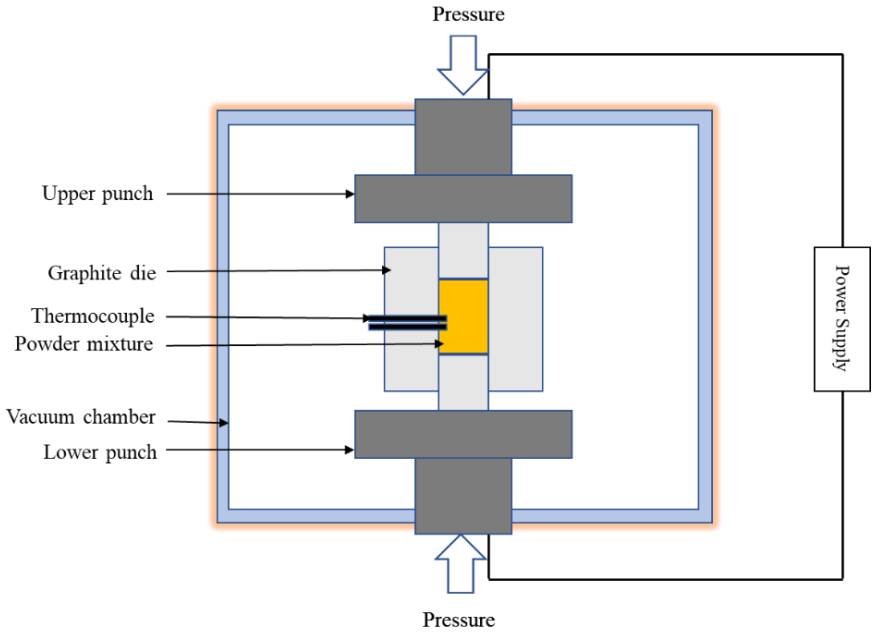

Fig 2.2 Schematic illustration of the spark plasma sintering equipment

The prepared mixture of powders is loaded in the cylindrical graphite die to prepare the composite of dimension 10×10 mm^3. After that, the die assembly is kept in the sintering chamber. The powders are sintered for 20 minutes at a pressure of 50Mpa and two different temperatures of 550°C and 575°C. The process is described by the sintering curves, which are displayed in Fig.2.3 All instances of sample manufacturing used the same procedures. Small variations were however possible because variables were manually controlled.

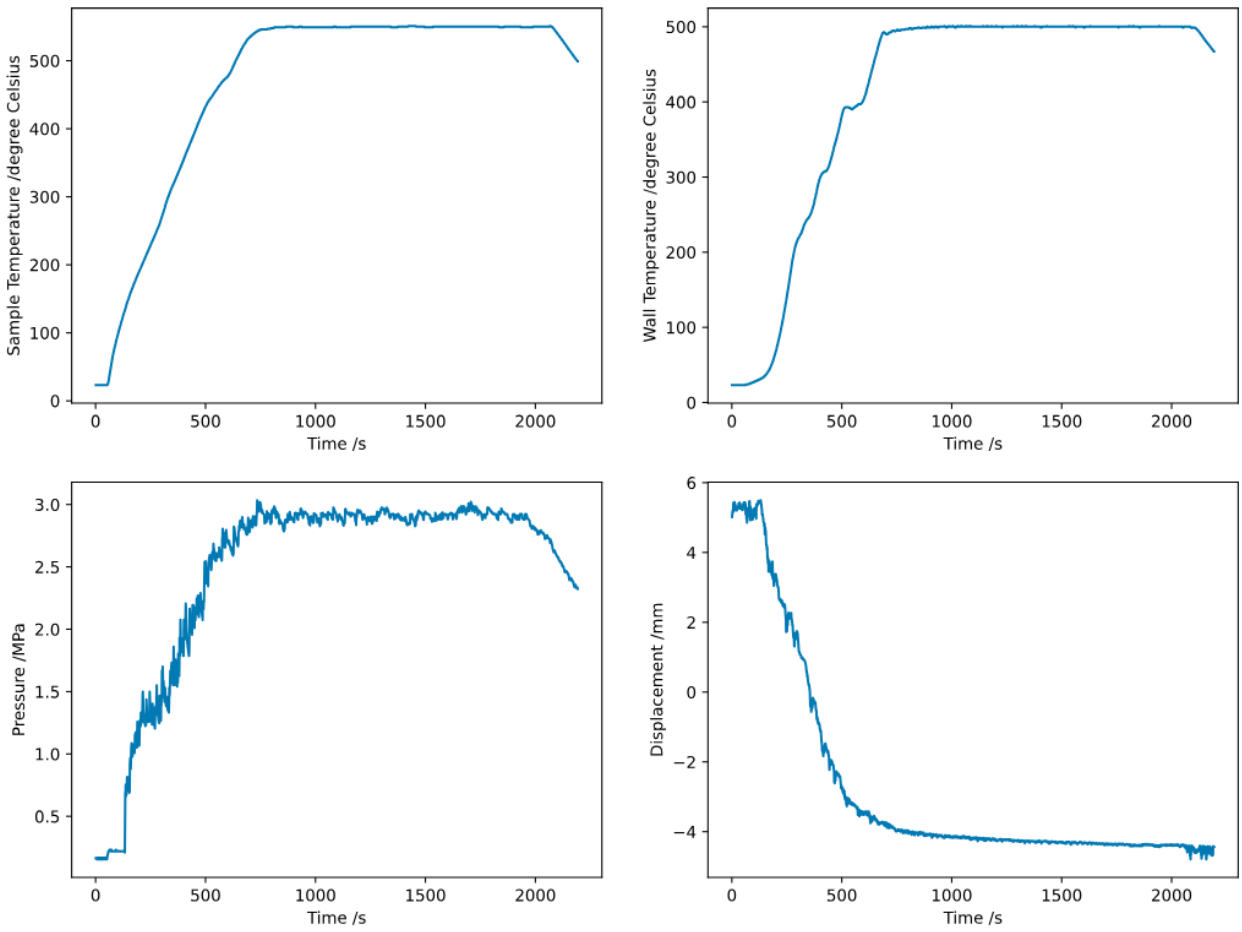

Fig 2.3 Sintering Curves of the fabricated specimen

2.6 Relative Density Measurement of Composite

Relative density or specific gravity is the ratio of the density of a substance to the density of a given reference material. Specific gravity usually means relative density with respect to water. Relative density of the substance is calculated using the Archimedes Principle. Relative density (RD) or specific gravity (SG) is a dimensionless quantity, as it is the ratio of either densities or weights, and it is calculated using the formula.

$$Relative\ Density = \frac{\rho_{substance}}{\rho_{reference}}$$

where RD is relative density, $\rho_{substance}$ is the density of the substance being measured, and $\rho_{reference}$ is the density of the reference. For each of the samples which were fabricated using the conventional sintering process, the relative density is measured by using the Archimedes Principle. Archimedes principle states that when a body is immersed completely or partially in a fluid, it experiences an upward force that is equal to the weight of the fluid displaced by the body. Since 1 ml of water has

a mass of almost exactly equal to 1 g, if the object is immersed in water, the difference between the two masses (in grams) will equal (almost exactly) the volume (in ml) of the object weighed.

The most common method for the determination of the density of solids is the immersion method. A specimen was weighed in air and its mass is being recorded. It was then immersed in a liquid and its apparent mass upon immersion is recorded. The specific gravity and density are then calculated. The immersion liquid can be either distilled water or ethanol. The theoretical density was calculated by dividing the mass of the powder used for production by the volume of a cylinder.

$$Relative\ Density = \frac{measured\ value}{theoretical\ density}$$

2.7 Optical Microscope Observation

Optical microscope (OM, OPTIPHOT-2, Nikon Co., Ltd.) was used to observe the microstructure of the specimens. The Al specimen and Al-CF specimen were grinded starting from 250 grit and polished up to 1200 grit. After grinding and polishing, the specimens were mirror-polished with a 3 μm and 1 μm diamond slurry. The specimens were then cleaned in acetone using an ultrasonic cleaner for 10 minutes. The morphology and texture were observed from the polished specimen using the optical microscope which uses the visible light and system of lens which generates the magnified images of the specimen.

2.8 Thermal Conductivity Measurement

Thermal conductivity often denoted by k, λ, or κ refers to the ability of a material to transfer or conduct heat. It is one of the three methods of heat transfer, the other two being convection and radiation [18]. Thermal conductivity is quantified using the SI unit of W/m•K (Watts per meter per degree Kelvin) and is the reciprocal of thermal resistivity, which measures the ability of an object to resist heat transfer. Thermal conductivity can be calculated using the following equation:

$$k = \frac{Q * L}{A(T2 - T1)}$$

Where L is the thickness of the material.

A is the Surface Area of the material.
Q is the Heat flow, and
T2-T1 is the Temperature Gradient.

The thermal conductivity of the sample was measured at room temperature and the sample was polished to 800 grit until the surface became flat. The sample of the dimensions φ10×10 mm was placed in the middle between the hot and cold bars. The top and bottom surface of the sample was applied with grease and kept between the hot and cold bars so that it can in be in contact with each other. Then the doctite paste which is the conductive paste was applied to the thermocouples of the

hot bar, cold bar, and the sample. After the sample was measured and the thermocouple setting was made, the heating plate was heated to room temperature + 5K, the cooling plate was cooled to room temperature -5K, and the temperature gradient between the heating plate and the cooling plate was set to 10K. After leaving the sample till it reaches the steady state, the temperature of each thermocouple was measured at 1 s intervals for 300 s. The temperature was recorded by the thermocouple recorder and data acquisition system. The length of the thermocouples connected to the sample using doctite was measured by Vernier Caliper. The experiment was conducted, and the data were acquired, and effective thermal conductivity was calculated using Fourier's law which is a basic law of heat conduction. The analysis was performed by using the software Terapad and Python.

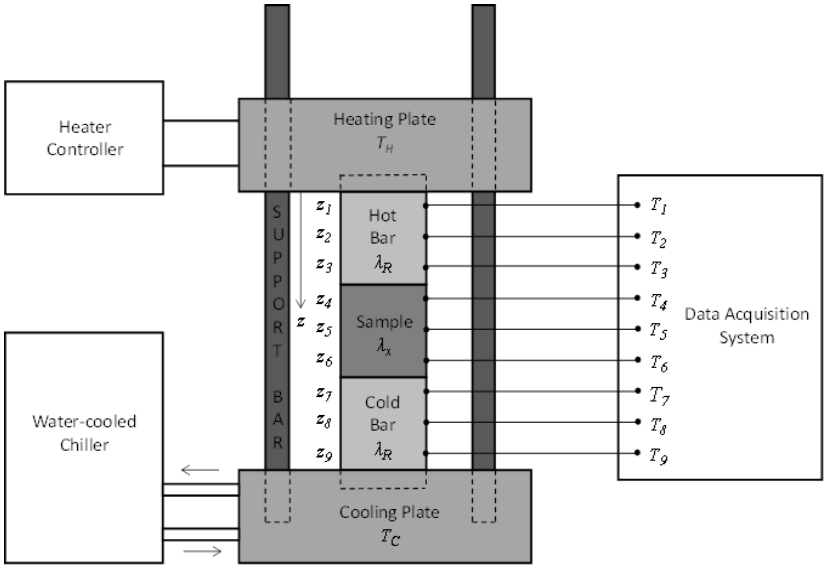

Fig 2.4 Thermal Conductivity Measurement Scheme.

The temperature gradient of each of the bar portions is a_h, $a_s$and a_c,

$$a_h = \sum_{i=1}^{3}(z_i - \bar{z}_h)(T_i - \bar{T}_h)/\sum_{i=1}^{3}(z_i - \bar{z}_h)^2, \bar{z}_h = \frac{1}{3}\sum_{i=1}^{3} z_i\,, \bar{T}_h = \frac{1}{3}\sum_{i=1}^{3} T_i$$

$$a_S = \sum_{i=4}^{6}(z_i - \bar{z}_s)(T_i - \bar{T}_s)/\sum_{i=4}^{6}(z_i - \bar{z}_h)^2, \bar{z}_h = \frac{1}{3}\sum_{i=4}^{6} z_i\,, \bar{T}_s = \frac{1}{3}\sum_{i=4}^{3} T_i$$

$$a_c = \sum_{i=7}^{9}(z_i - \bar{z}_c)(T_i - \bar{T}_c)/\sum_{i=7}^{9}(z_i - \bar{z}_c)^2, \bar{z}_c = \frac{1}{3}\sum_{i=7}^{9} z_i\,, \bar{T}_c = \frac{1}{3}\sum_{i=7}^{9} T_i$$

We can obtain the effective thermal conductivity of the measurement sample as:

$$\boldsymbol{\lambda}_x = \frac{\boldsymbol{\lambda}_x(a_h - a_c)}{2a_s}$$

2.9 Vickers Hardness Testing

The Vickers hardness was used to check the hardness of the material using a square-based diamond pyramid indenter. The indenter was pressed into the surface of the material by slowly applying a known load and the resulting impression was measured mechanically or optically. A large impression for a given load and indenter indicates a soft material and a smaller impression indicates a hard material. The indenter was forced into the surface of the material under the action of 300g for 15 seconds at five random points. Considering Aluminum is a softer material, the load has been taken to be 300g. The view of the impression was checked through the microscope and the noted values are calculated using the conversion tables. The unit of hardness by this method is the diamond-pyramid hardness number (DPH) or Vickers hardness number (VHN). It is defined as the applied load divided by the surface area of indentation.

$$VHN = \frac{Applied\ Load}{Surface\ Area\ of\ impression} = \frac{2Psin\frac{\theta}{2}}{D^2} = \frac{18544\,P}{D^2},$$

Where, $\theta = 136°$

P is the applied load in kg,

θ is the angle between the opposite faces of diamond, And D is the mean diagonal length in mm.

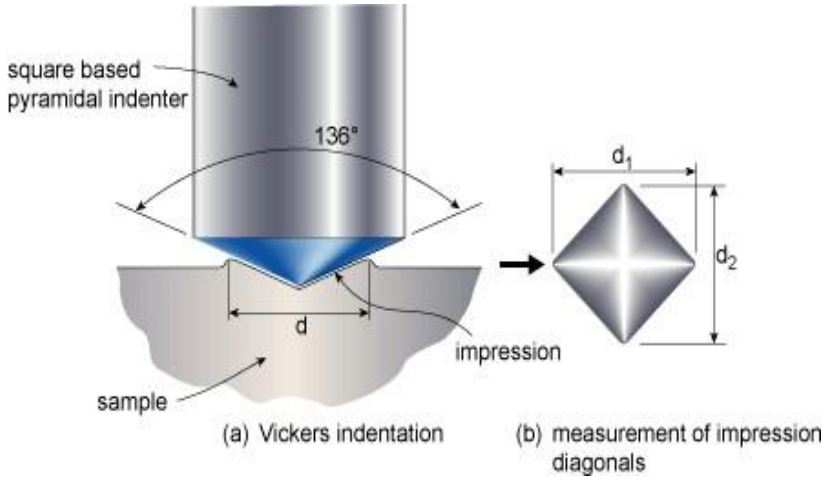

Fig 2.5 Vickers Hardness Testing Scheme.

Chapter 3 Results and Discussion

Al powder and CF powder were used as the raw materials for the preparation of the composite. At first, Ultrasonic cleaning was done on carbon fibers to prevent agglomeration and re-bonding. Then the CF was mixed with Al powder using pot mill rotating table for different rotation speed. The mixture of the CF and Al were fabricated by spark plasma sintering to obtain the composites. Surface properties like microstructure observation was carried out in the composite and the same composite was used to investigate about the mechanical properties like relative density, thermal conductivity, and Vickers hardness.

3.1 Dispersibility

To experimentally measure the uniform dispersion, the quantitative method known as dispersibility is used. The carbon fiber distribution was counted and then image processing techniques such as binary image conversion, filtering, thresholding, and noise reduction.
LN2D method is used to evaluate the spatial distribution of second phase particles. Initially, the number of gravity centers (GCs) of second phase particles in the measuring circle, in which the center is located at GC of a identified particle (LN2D), or at several random locations (LN2DR).

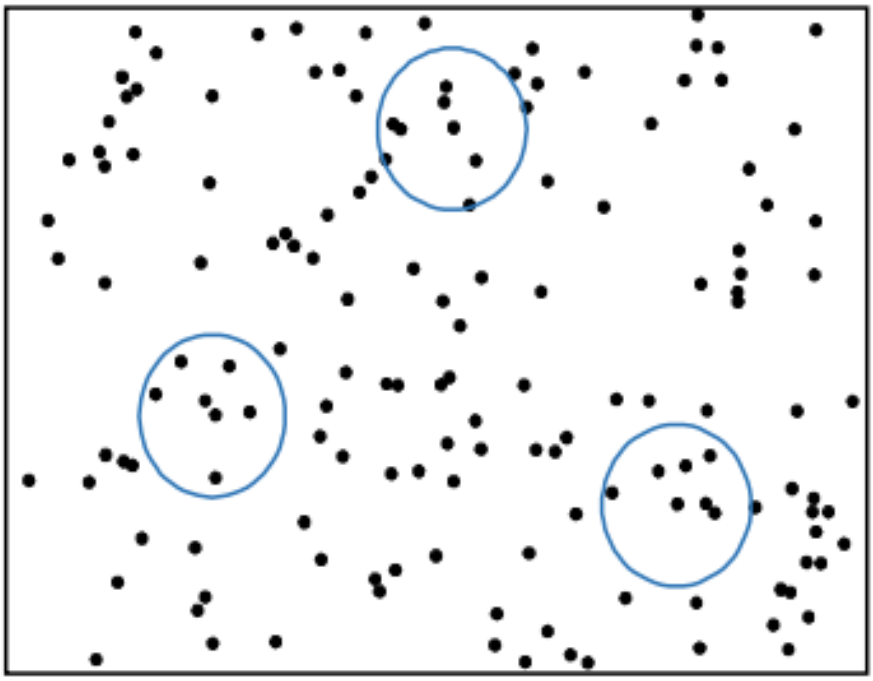

Fig. 3.1 Local Number 2-Dimensional model diagram.

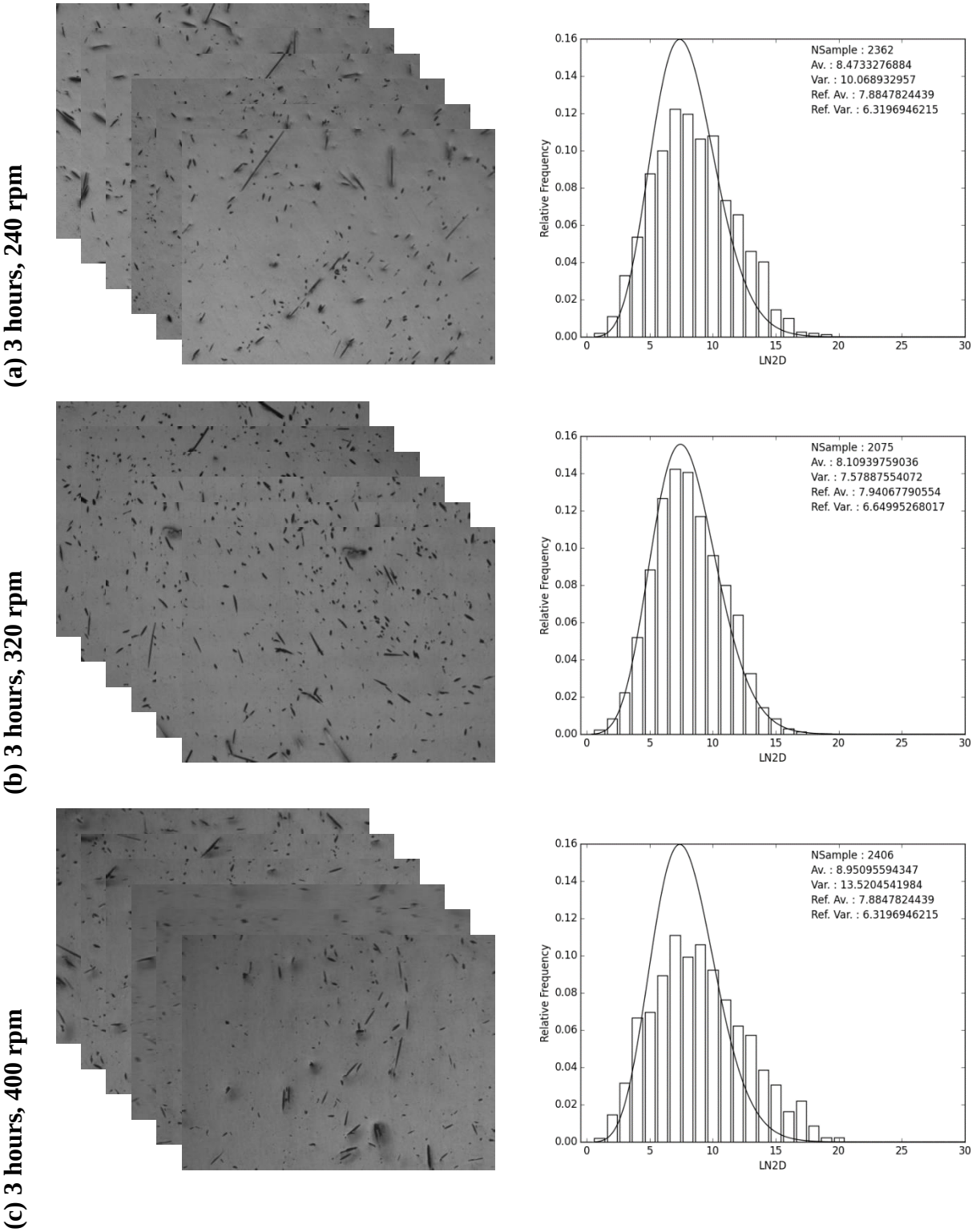

Fig. 3.2 OM and LN2D images of samples with different mixing conditions.

From figure 3.2 (a)- (c) indicates the OM images of samples fabricated with three different mixing conditions such as 240, 320, and 400 rpm for 3 hours. The samples were observed through Optical microscopy technique and series of images were obtained. These images were then fed as input to the LN2D application. The relative frequency spectrum vs LN2D were obtained as output. We used series of 10 images as input for this analysis. The results with 320 rpm sample have a Var. value of 7.5788 which is the least among the other samples at different mixing conditions. The least value indicates that it has good random distribution of the reinforcement.

3.2 Relative density

Mechanisms that take place during increase in temperature are the particle rearrangement, localized and bulk deformation. These mechanisms can affect the microstructure and mechanical properties of the sintered samples, especially densification. The density of Aluminum is 2.7 g/cm^3 and the density of carbon fiber (CF) is 2 g/cm^3.The relative density of the specimen samples are measured by the Archimedes Principle and the measured density values is shown in table 3.1. The theoretical density was calculated for each powder mixture based on the rule of mixtures approach as shown by the equation:

$$\rho_{th} = \rho_m V_m + \rho_{r.f}\ V_{rf}$$

Where ρ_m and $\rho_{r.f}$ are the densities of the matrix and the reinforcement respectively and V_m and $V_{r.f}$ are the volume fraction of the matrix and reinforcement respectively. The theoretical density of 1% and 2% of CF/Al composite are 2.695 g/cm^3 and 2.69 g/cm^3.

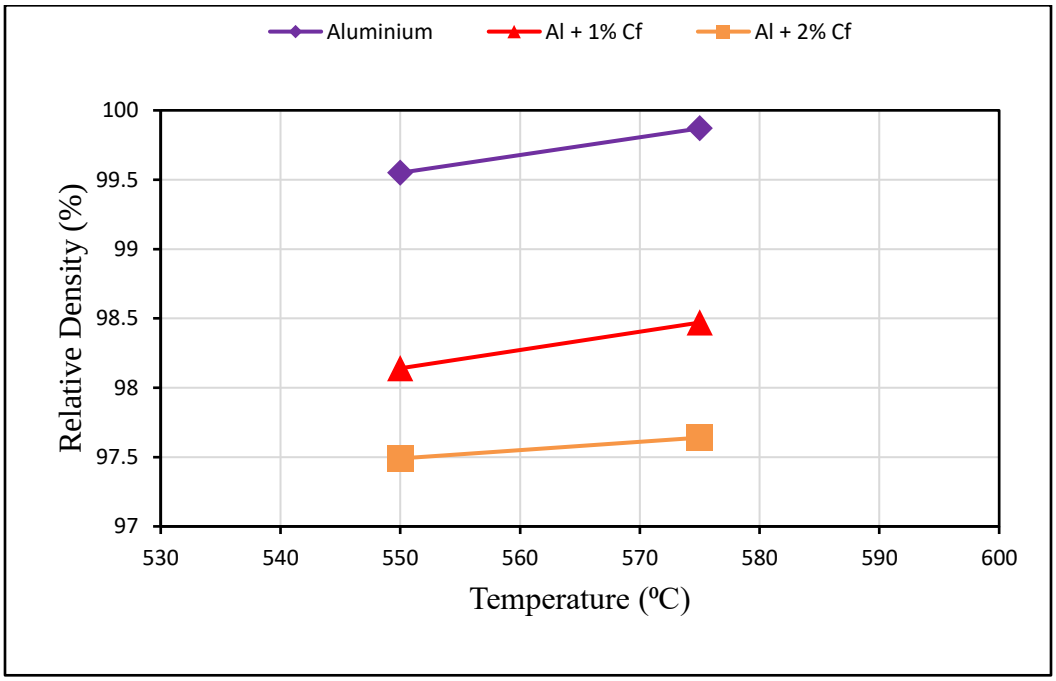

Fig. 3.3 Relative density of the composites in graphical representation

Table 3.1 Relative density of the SPS fabricated composites.

Sample	Temperature	Relative Density
Aluminum	At 550℃	99.55
Aluminum	At 575℃	99.87
Al + 1% CF	At 550℃	98.14
Al + 1 % CF	At 575℃	98.47
Al + 2 % CF	At 550℃	97.49
Al + 2 % CF	At 575℃	97.64

From the figure 3.3 and Table 3.1, it is clear that since the relative density values are higher than 97.49%, the sintering effects of the samples were good. The relative density values increase with increase in fabrication temperature. This is due to the evolution of grain boundaries between Al particles which helps to eliminate the pores in the sample.

3.3 Microstructure observation – OM

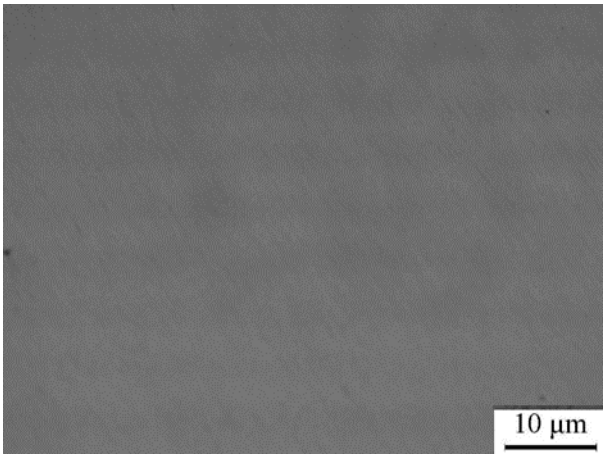

Fig. 3.4 OM images of Al block - 550℃.

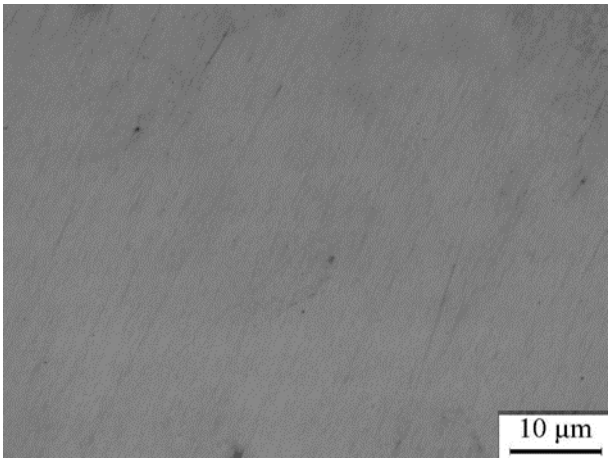

Fig. 3.8 OM images of Al block - 575℃.

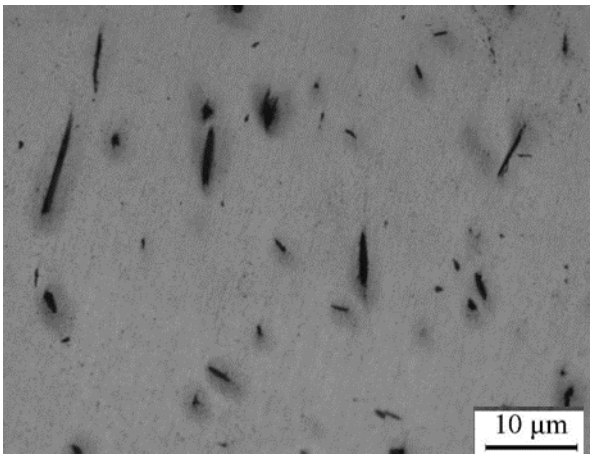

Fig. 3.5 OM images of 1% CF/Al composite- 550℃.

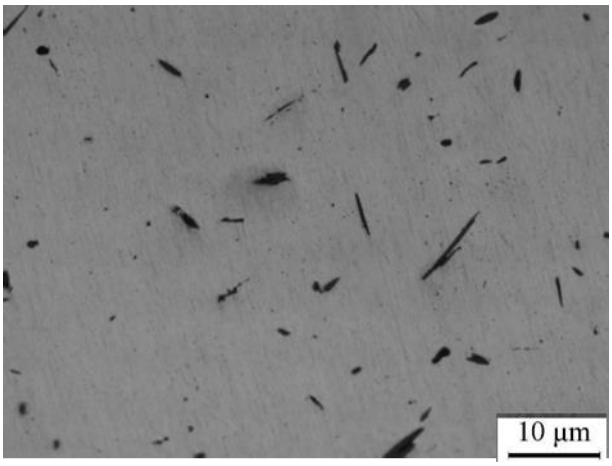

Fig. 3.9 OM images of 1% CF/Al composite- 575℃.

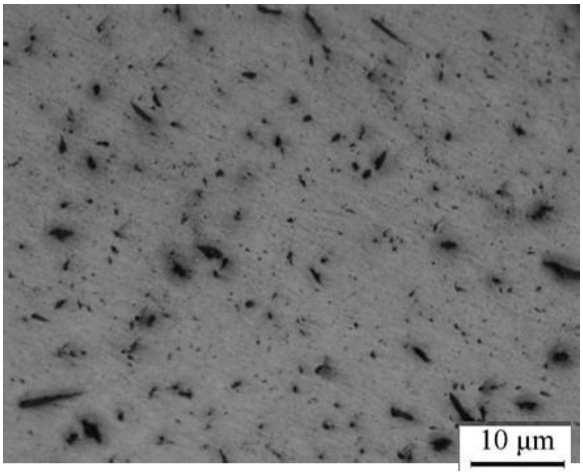

Fig. 3.6 OM images of 2% CF/Al composite- 550℃.

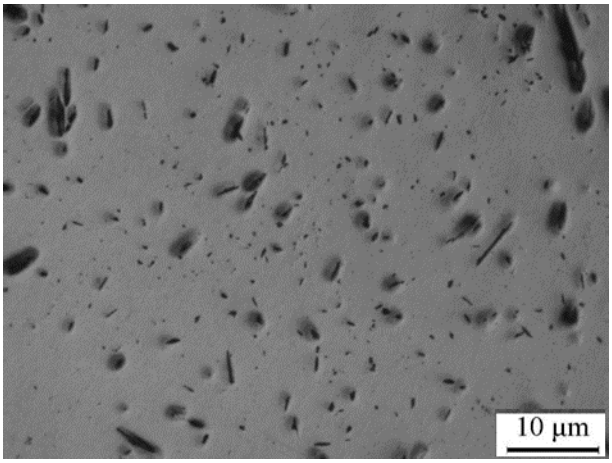

Fig. 3.10 OM images of 2% CF/Al composite- 575℃.

From the figure 3.4 to 3.10, the OM images of Al block, 1% and 2% of CF/Al composite at 550℃ and 575℃ respectively. The composite shows different appearances of Al (grey region) and CF (black region) and it indicates dispersed CF in the Al matrix. Figure 3.5 -3.6 shows particle size reduction of CF from the effect of ball milling, the breakdown of CFs occurred due to the mechanical forces generated by the collision of grinding balls and the material itself.

Figure 3.5 and 3.10 shows the CFs the widely distributed across the matrix with the increase in CF volume fraction, and leads to some agglomeration. This results in increase of pores between Al and CF which further leads to the decrease in relative density of the composite. In both fabrication temperature, as there is increase in volume fraction shows the random particle size reduction of the reinforcement which occurred due to the breakage of reinforcement during ball milling of the mixture.

3.4 Measurement of Thermal conductivity

The thermal conductivity of all the samples were measured and compared to understand the relationship with fabrication temperature and the volume fraction as shown in figure 3.11 - 3.16. Increasing the fabrication temperature from 550℃ to 575℃ results in the increase of thermal conductivity. But the experimental value is lower than the theoretical thermal conductivity of the composite (rule of mixtures) which is clearly evident based on figure 3.15 and 3.16. It was contributed by the porosity and thermal resistance at the Al/CF interface layer. In general, the reinforcement of carbon fiber will result in improving the thermal conductivity but the measured value from the experiments shows the thermal conductivity decreased with increasing the carbon fiber content. This may be due to anisotropy of the reinforcement and the heat cannot flow in one direction. Depending on the arrangement of the reinforcement, the thermal conductivity can vary significantly along different axes, So increasing the carbon fiber content results in the increased random orientation and a non-uniform size of the fiber which hinders the thermal conductivity

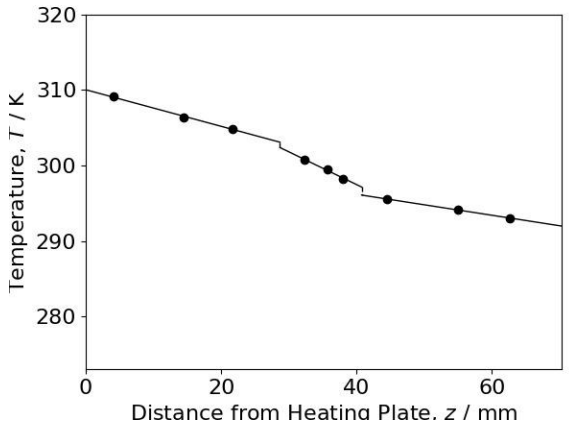

Fig. 3.11 Pure Al – 700℃ Experimental TC

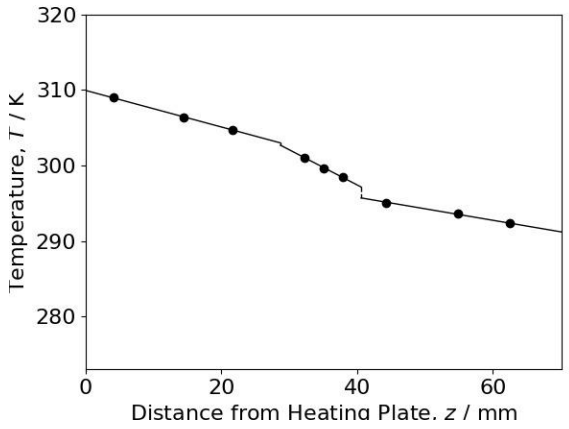

Fig. 3.12 Al+1% – 575℃ Experimental TC

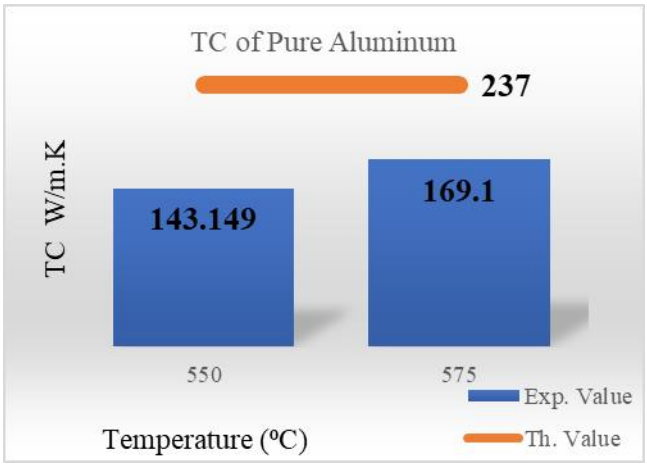

Fig. 3.14 Comparison of TC of Pure aluminum

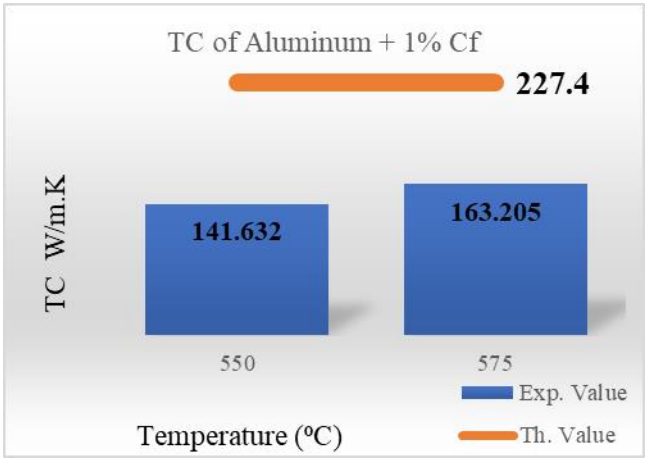

Fig. 3.15 Comparison of TC of 1% CF/Al composite

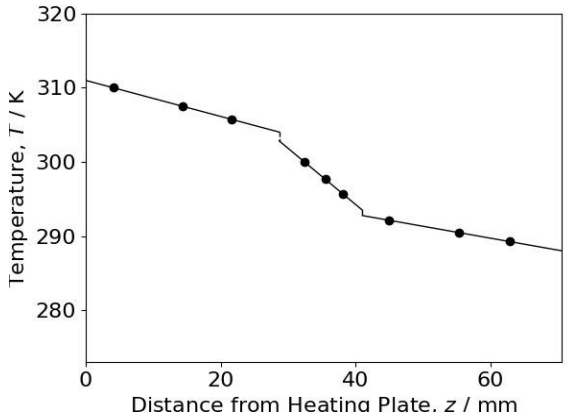

Fig. 3.13 Al+2% – 575°C Experimental TC

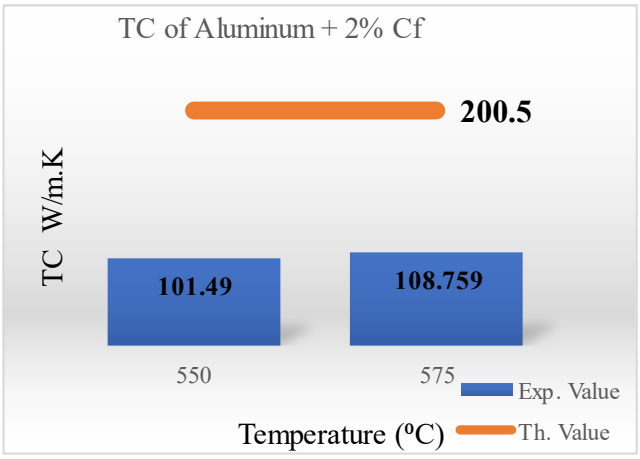

Fig. 3.16 Comparison of TC of 2% CF/Al composite

3.5 Theoretical Thermal conductivity

A more generalized equation for a two-dimensional steady state heat flow is provided by the theoretical approach. Different theoretical methods, such as the rules of mixture approach and the finite volume approach, can be used to determine the thermal conductivity of composites in order to estimate the heat flow in anisotropic composite materials in any direction. Maxwell's Mixing Rule to estimate the effective thermal conductivity of the composite based on the thermal conductivities of its individual constituents (aluminum and carbon fiber) and their volume fractions.

The Maxwell's Mixing Rule assumes that the composite consists of two distinct phases (aluminum and carbon fiber), and the overall thermal conductivity is determined by their volume fractions and individual thermal conductivities.

The equation for estimating the effective thermal conductivity (K_{eff}) of the composite is as follows:

$$K_{eff} = V_{Al} * k_{Al} + V_{cf} * k_{cf}$$

where, K_{eff} is the effective thermal conductivity of the composite.

V_{Al} is the volume fraction of aluminum in the composite.

k_{Al} is the thermal conductivity of pure aluminum.

V_{cf} is the volume fraction of carbon fiber in the composite.

k_{cf} is the thermal conductivity of carbon fiber.

The thermal conductivity of 1% and 2% CF/Al composite calculated from the rules of mixture is 240.13 W/m•K and 243.26 W/m•K.

One more approach is that, to eliminate the effect of the pores on thermal conductivity, the following equation derived by Landauer was employed.

$$K_{Al-eff} = \frac{1}{4}\left[K_p(3V_p - 1) + K_{Al}(3V_{Al} - 1) + ([K_p(3V_p - 1) + K_{Al}(3V_{Al} - 1)]^2 + 8K_pK_{Al})^{1/2}\right]$$

Where K_{Al-eff} denotes the effective thermal conductivity of Al matrix; K_{Al} and K_p denote the thermal conductivity of aluminum and air, respectively. V_{Al} and V_p are the volume fractions which are in relation with respect to the relative density. The orientation of the fiber is also necessary to calculate the theoretical thermal conductivity of the composite.

The thermal conductivity of fiber is highly anisotropic, which can be extended to estimate the thermal conductivity which is parallel to the fiber direction ($K_{||}$) using the equation below:

$$K_{||} = K_a\left[1 - \left(1 - \frac{K_c}{K_a}\right) sin^2 Ø\right]$$

Where K_a and K_c is the thermal conductivity along the fiber axis and the thermal conductivity perpendicular to the fiber axis and Ø is the fiber angle.

The thermal conductivity of 1% and 2% CF/Al composite calculated using this approach is 224.7 W/m•K and 200.5 W/m•K.

3.6 Relationship between Relative density and thermal conductivity

One of the most notable revelations is the inverse relationship between the volume fraction of carbon fiber and both the thermal conductivity and relative density of the composite. As the carbon fiber content increases, there appears to be a concurrent decrease in both thermal conductivity and relative density. This counterintuitive observation could be attributed to the random orientation and non-uniform size of the carbon fibers within the composite. These irregularities might disrupt the smooth transfer of heat, leading to a reduction in thermal conductivity. Additionally, the presence of carbon fibers could introduce voids or porosity, thereby contributing to a decrease in the composite's relative density.

Conversely, the study underscores the positive correlation between fabrication temperature and both relative density and thermal conductivity. This relationship suggests that higher fabrication temperatures foster an environment conducive to enhanced particle rearrangement and improved interatomic contacts. Consequently, as the relative density of the material increases, any inherent porosity or voids are minimized. This reduction in voids allows for more efficient phonon transport through the composite material, resulting in an increase in thermal conductivity. In essence, the rise in fabrication temperature seems to contribute to a more tightly packed composite structure with

fewer imperfections, thus facilitating better thermal conduction.

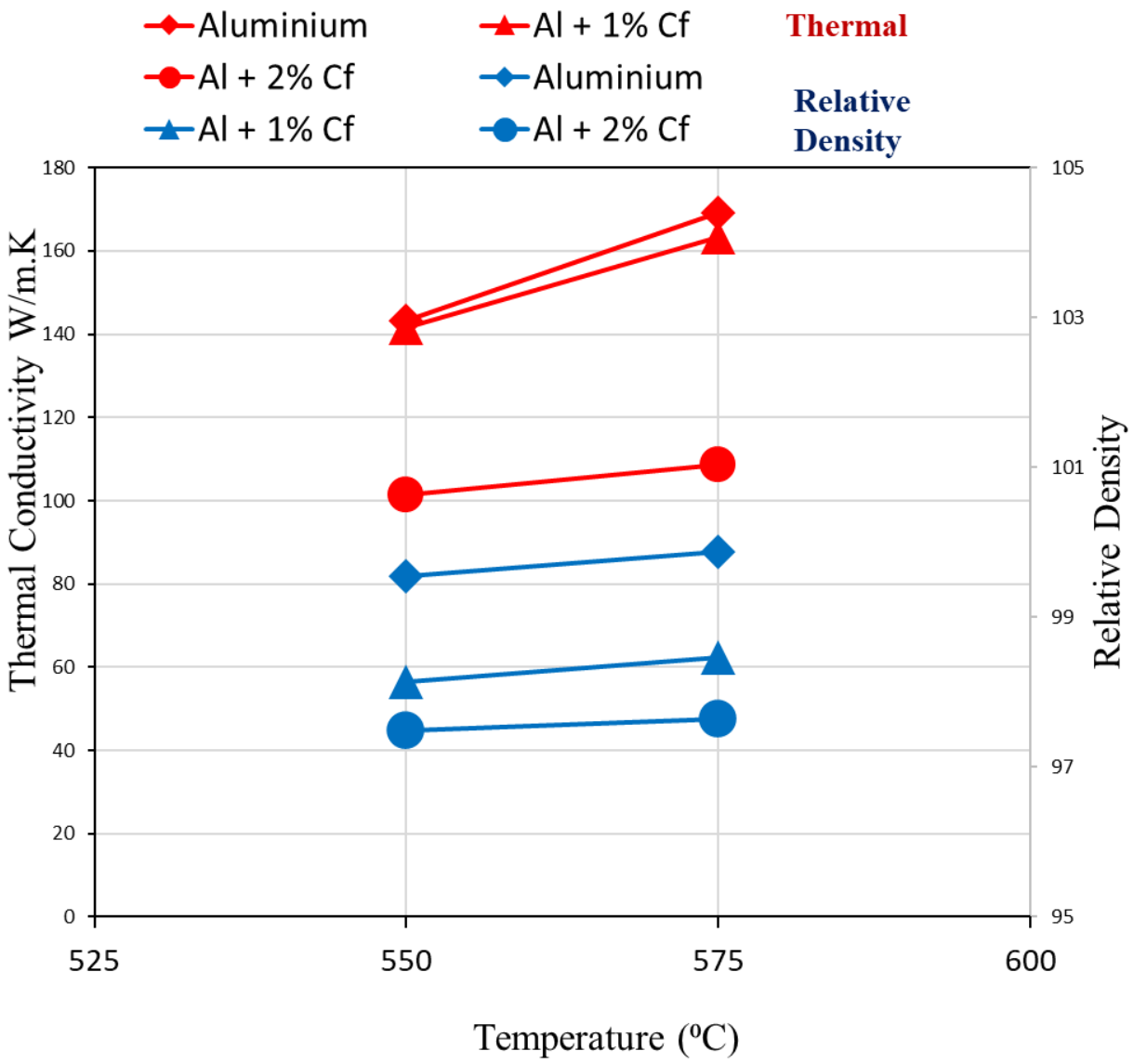

Fig. 3.17 Thermal conductivity and relative density relationship

3.7 Vickers Harness

According to the load transfer mechanism, reinforcing fibers, such as carbon fibers, are typically much stronger and stiffer than Al. When a load is applied to the composite, the fibers bear a significant portion of the load due to their high strength, effectively transferring the stress from the matrix to the fibers. As the volume fraction of fibers increases, more load is transferred to the fibers, leading to higher hardness and improved mechanical properties as shown in figure 3.18 and 3.19. As the sintering temperature rises, the hardness of the composite decreases, this is due to the phenomenon called “softening” which occurs in many metals including aluminum as shown in figure 3.19.

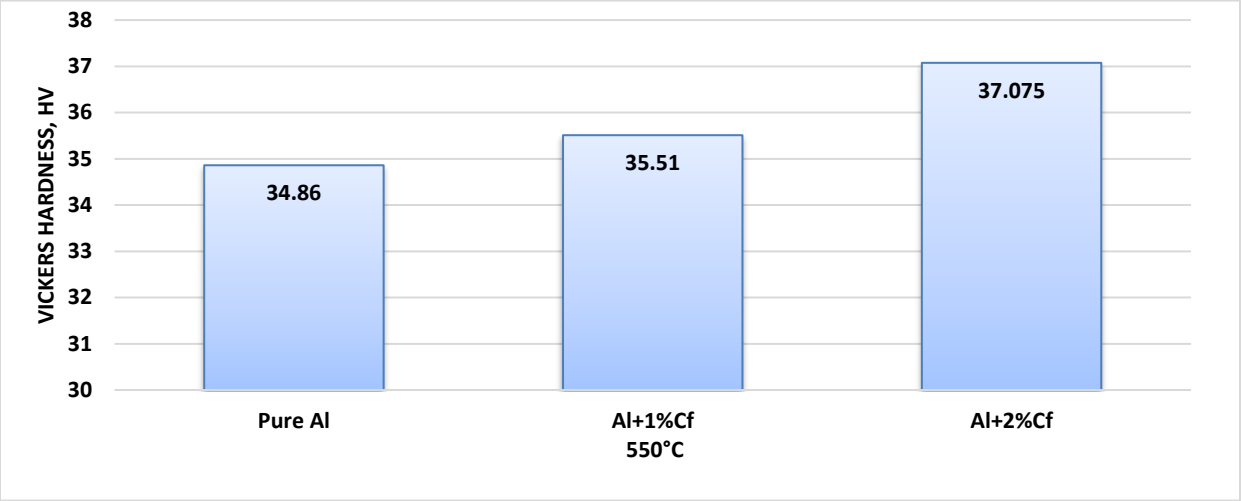

Fig. 3.18 Vickers hardness comparison of CF/Al composites fabricated at 550℃

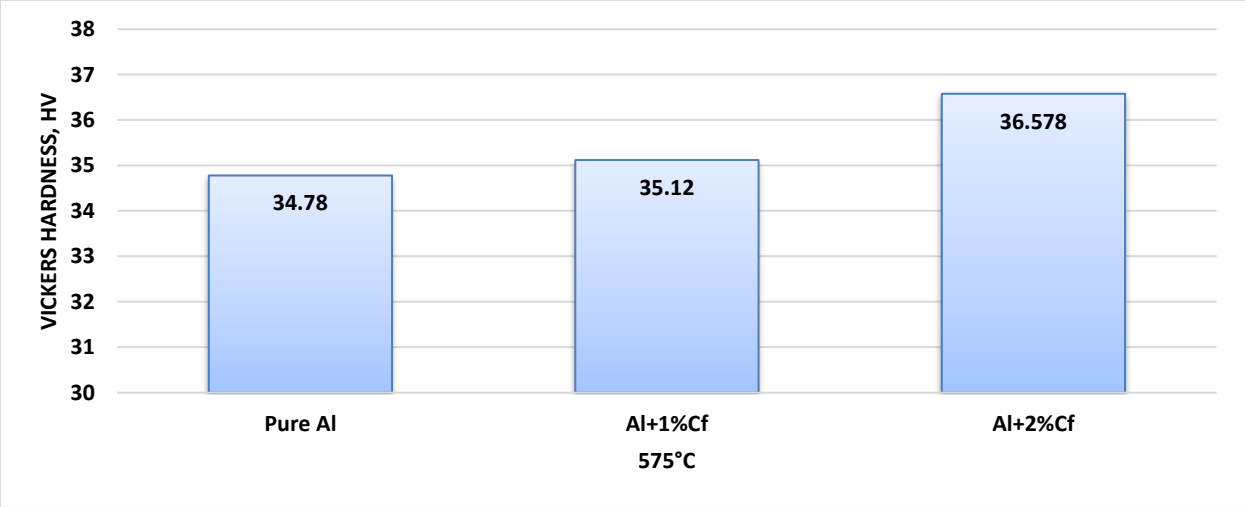

Fig. 3.19 Vickers hardness comparison of CF/Al composites fabricated at 575℃

Chapter 4 Conclusion

CF dispersed pure Al composites were fabricated by spark plasma sintering process. In this study, we focused on the issues faced by mixing conditions, CF dispersion, and the temperature effect on the properties of the composites.

The significant results obtained are summarized below:

Ball Milling Time and Reinforcement Dispersion:

- The study found that the duration of ball milling significantly affects how well the carbon fiber reinforcement is dispersed within the aluminum matrix.
- Effective ball milling rpm likely leads to better dispersion of carbon fibers throughout the aluminum matrix, which can have positive effects on the mechanical and thermal properties of the composite.
- Proper dispersion is important to ensure effective load transfer and reinforcement of the composite material.

Fabrication Temperature and Relative Density:

- Increasing the fabrication temperature during the spark plasma sintering process leads to higher relative density of the composite.
- Higher temperatures likely promote better particle rearrangement and bonding between aluminum and carbon fiber, resulting in a denser composite structure.
- A denser structure can have implications for the mechanical properties, thermal conductivity, and overall performance of the composite.

Thermal Conductivity and Reinforcement Volume Fraction:

- The study observed that thermal conductivity decreases as the volume fraction of carbon fiber reinforcement increases.
- This counterintuitive trend might be attributed to the random orientation and non-uniform size of the carbon fibers.
- Non-uniform distribution and orientation of the carbon fibers can disrupt the efficient flow of heat through the material, leading to a reduction in thermal conductivity.

Hardness and Carbon Fiber Content:

- The hardness of the composite material increases with higher carbon fiber content.
- This is likely due to the load transfer mechanism, where the stiff carbon fibers contribute to the composite's overall hardness.
- The carbon fibers effectively share some of the mechanical load with the aluminum matrix.

Fabrication Temperature and Hardness:

- The hardness of the composite material decreases as the fabrication temperature increases.
- This phenomenon is referred to as "softening" and could be attributed to various factors, including possible changes in microstructure, grain growth, or recrystallization of the material at elevated temperatures.

References

[1] Teiichi Inada: Thermal Management Materials: Hitachi Chemical Technical Report, 54 (2011).

[2] Saums, D: "Vehicle Electrification Thermal Management Challenges and Solutions Overview", MEPTEC Thermal Management Workshop, San Jose CA USA, (March 2011).

[3] M. K. Surappa: Aluminium matrix composites: Challenges and opportunities: 28, (2003).

[4] K. C. Chang, K. Matsugi, G. Sasaki and O. Yanagisawa: JSME Int. J. 48 (2005) 205–209.

[5] K. C. Chang, K. Matsugi, G. Sasaki and O. Yanagisawa: J. Japan Inst. Metals 69 (2005) 983–988.

[6] Carbon Nanofibers and Their Composites: A Review of Synthesizing, Properties and Applications: LichaoFeng, NingXie, and Jing Zhong: Materials 2014, 7, 3919-3945; doi:10.3390/ma7053919.

[7] Khorshid MT, Jahronmi SJ, Moshksar M (2010) Mechanical properties of tri-modal Al matrix composites reinforced by nano and submicron sized al203 particulates by wet attrition milling and hot extrusion. Mater Des 31:3880-3884.

[8] Show Denko Co., Ltd., Material Safety Data Sheet, (2007) p. 1.

[9] Casati R, Bonollo F, Dellasaga D, Fabrizi A, Timelli G, Tuissi A, Vedani M (2014) ex situ Al-Al_2O_3 ultrafine grained nanocomposites produced via power metallurgy. J alloy compd 615: S386-S388.

[10] X. H. Qu, L. Zhang, M. Wu and S. B. Ren: Prog. Nat. Sci. 21 (2011) 189-197.

[11] U. K. G. B. Annigeri Veeresh Kumar: Materials Today: Proceedings 4 (2017) 1140-1146.

[12] K. Mizuuchi, K. Inoue and Y. Agari: Microelectronics Reliability 79 (2017) 5- 19. [17] X. H. Qu, L. Zhang, M. Wu and S. B. Ren: Prog. Nat. Sci. 21 (2011) 189-197. [18] D. B. Miracle: Compos Sci Technol 65 (2005) 2526-2540

[13] K. Shirvanimoghaddam, S. U. Hamim, M. Karbalaei Akbari, S. M. Fakhrhoseini, H. Khayyam, A. H. Pakseresht, E. Ghasali, M. Zabet, K. S. Munir, S. Jia, J. P. Davim and M. Naebe: Composites Part A: Applied Science and Manufacturing 92 (2017) 70- 96.

[14] S. C. Tjong: Materials Science and Engineering: R: Reports 74 (2013) 281-350.

[15] J. G. Santanach, A. Weibel, C. Estournes, Q. Yang, C. Laurent and A. Peigney: Acta Mater 59 (2011) 1400-1408.

[16] ZheFeng Xu, Yong-Bum Choi, Kazuhiro Matsugi, Dong-Chun Li and Gen Sasaki: Materials Transactions, Vol. 50, No. 9 (2009) pp. 2160 to 2164.

[17] N. Saheb et al., "Spark plasma sintering of metals and metal matrix nanocomposites: A review," J. Nanomater., vol. 2012, 2012, doi: 10.1155/2012/983470.

[18] M. Wang *et al.*, "Hot rolling behavior of graphene/Cu composites," *J. Alloys Compd.*, vol. 816, p. 153204, Mar. 2020, doi: 10.1016/J.JALLCOM.2019.153204

Acknowledgements

First, I would like to extend my sincere and heartful obligation to all persons who have helped me and for their support starting from my entry to Japan, enrollment in Hiroshima University and for also my future career in Japan. Without their active guidance, help and encouragement I would not have made the progress in Japan.

I am extremely thankful and pay my gratitude to Gen Sasaki, Professor, Material Physics Laboratory, for his valuable guidance, support, encouragement, and keen interest, which helped me throughout this study.

I am also greatly indebted to Kenjiro Sugio, Associate Professor, Material Physics Laboratory, for the support, encouragement, and positive help and in clarifying the doubts about the machine and subjects.

I convey my sincere gratitude to Toru Takashina, Professor, Hiroshima University. Without his proper guidance and direction, I would not have completed my job-hunting process and his support helped me to get my job in Horkos, a CNC machine manufacturing company in Fukuyama, Japan.

I also extend our sincere thanks to our present and past lab mates and friends of Material Physics Laboratory and Property Control of Material Laboratory in Department of Mechanical Science and Engineering for their encouragement and continuous support they showed to me for my both personal and student life.

Finally, I express my gratitude to Hiroshima University, Japan for giving me an excellent opportunity to pursue my studies.